Regional seismic loss estimation and critical earthquake scenarios for the Western Quebec seismic zone

Katsuichiro Goda, Jeremy Rimando, Alexander L. Peace, Navid Sirous, Philippe Rosset & Luc Chouinard

View supplementary material 🗗

Published online: 17 Apr 2023.

Submit your article to this journal 🗗

View related articles 🗗

View Crossmark data 🗗

Taylor & Francis
Taylor & Francis Group

Check for updates

RESEARCH ARTICLE

Regional seismic loss estimation and critical earthquake scenarios for the Western Quebec seismic zone

Katsuichiro Goda[a,b], Jeremy Rimando [c], Alexander L. Peace [c], Navid Sirous[a], Philippe Rosset [d] and Luc Chouinard[d]

[a]Department of Earth Sciences, Western University, London, Canada; [b]Department of Statistical and Actuarial Sciences, Western University, London, Canada; [c]School of Earth, Environment & Society, McMaster University, Hamilton, Canada; [d]Department of Civil Engineering, McGill University, Montreal, Canada

ABSTRACT
Earthquakes pose potentially substantial risks to residents in the Western Quebec seismic zone of eastern Canada, where Ottawa and Montreal are located. In eastern Canada, the majority of houses are not constructed to modern seismic standards and most homeowners do not purchase earthquake insurance for their homes. If a devastating earthquake strikes, homeowners would be left unprotected financially. To quantify financial risks to homeowners in the Western Quebec seismic zone, regional earthquake catastrophe models are developed by incorporating up-to-date public information on hazard, exposure and vulnerability. The developed catastrophe models can quantify the expected and upper-tail financial seismic risks by considering a comprehensive list of possible seismic events as well as critical earthquake scenarios based on the latest geological data in the region. The results indicate that regional seismic losses could reach several tens of billions of dollars if a moderate-to-large earthquake occurs near urban centres in the region, such as Montreal and Ottawa. The regional seismic loss estimates produced in this study are useful for informing earthquake risk management strategies, including earthquake insurance and disaster relief policies.

1. Introduction

Seismic hazard in Canada largely focuses on the Pacific coast where plate-boundary subduction processes have a high potential to produce large and frequent earthquakes (Hyndman and Rogers 2010). However, a potentially substantial and underappreciated seismic risk exists in the intraplate region of the Saint Lawrence rift system, where 25–30% of the Canadian population live and many houses are neither seismically designed nor constructed (Adams et al. 2002). Therefore, the impact of devastating earthquakes will be significant socioeconomically as well as financially. Historically, major damaging events of up to earthquake magnitude (M) 7.0 occurred in the Charlevoix seismic zone in 1663, 1791, 1860, 1870, 1925 and 1971, while moderate earthquakes of up to M6.2 occurred in the Western Quebec seismic zone (WQSZ) in 1732, 1935, 1944 and 2010, where Ottawa and Montreal are situated (Cassidy et al. 2010). Figure 1 shows historical seismicity in eastern Canada based on the Seismic Hazard Earthquake Epicentre File (SHEEF) catalog up to 2008 (Halchuk 2009) and the Canadian earthquakes archive data between 2009

and 2019 (https://open.canada.ca/data/en/dataset/4cedd37e-0023-41fe-8eff-bea45385e469).

Currently, potential earthquake ruptures in the Saint Lawrence region are poorly defined as ad-hoc, historical scenarios without specifying candidate geological faults. New geological evidence and geophysical modelling can play a critical role in improving the earthquake source characterisation (Morell et al. 2020). Recently, Lamontagne et al. (2020) created a comprehensive map of geological/geophysical lineaments that potentially represent pre-existing faults that may be capable of hosting future moderate-to-large earthquakes in the WQSZ. Building upon the new fault database, Rimando and Peace (2021) performed numerical stress modelling of these lineaments and showed that NNW- to NW-trending faults exhibit the highest slip tendency values and are therefore presently more likely to be reactivated. By combining these potentially active fault data with the stochastic earthquake source modelling (Goda 2017), it is possible to provide a sound foundation for future seismic hazard and risk assessments in the WQSZ.

A recent study by AIR Worldwide (2013) highlighted that the overall loss of 61 billion Canadian dollars (C$)
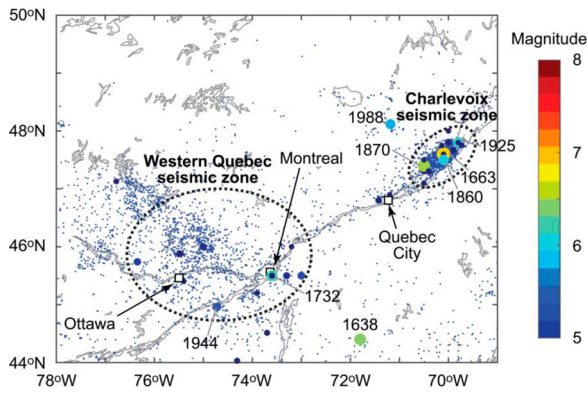
Figure 1. Map of the Saint Lawrence region and historical seismicity data based on the SHEEF catalog and the Canadian earthquakes archive database. Numbers indicated on the map are calendar years of major earthquakes in the region.

could occur due to a possible M7.1 earthquake in the Ottawa-Montreal-Quebec City corridor. For Montreal, Yu, Rosset, and Chouinard (2016) performed a seismic risk assessment for residential buildings at the census tract level using a set of seismic scenarios, whereas Rosset et al. (2019, 2022) extended the analysis to the metropolitan region by considering a finer spatial scale of dissemination areas. These studies were unique in integrating local building information as well as seismic microzonation information (Rosset and Chouinard 2009; Rosset, Bour-Belvaux, and Chouinard 2015). However, these were based on deterministic scenarios, similar to the ones proposed by Ghofrani et al. (2015) and were therefore not adequate to evaluate an exceedance probability (EP) loss curve of a regional building portfolio (i.e. a group of buildings) that requires the consideration of a comprehensive list of possible earthquake scenarios and their occurrence probabilities. In contrast, Goda (2019) conducted nationwide seismic risk assessments of single-family wooden houses in Canada and evaluated EP loss curves at individual locations. Although the individual assessments can be aggregated in terms of annual expected loss at a regional level, the right-tail risks of a building portfolio at a regional scale cannot be obtained because the assessments lack proper consideration of correlation in the estimated losses at individual locations. From disaster risk management perspectives, new quantitative earthquake risk assessments in Canada, enabled by nationwide building exposure models and seismic vulnerability models developed by the Geological Survey of Canada (GSC) through the Open Disaster Risk Reduction (OpenDRR) programme (https://opendrr. github.io/downloads/en/), will be valuable in establishing some objective basis for evaluating different options of disaster risk reduction measures.

This study aims to develop regional seismic risk models using the latest datasets and models for hazard, exposure and vulnerability, and to quantify the financial risks for homeowners in eastern Canada. In this paper, we focus on the WQSZ and carry out quantitative seismic risk assessments by evaluating EP curves. The seismic hazard model is based on the historical and regional seismicity models developed by the GSC (Halchuk et al. 2014; Kolaj et al. 2020), combined with different ground motion models (Atkinson and Adams 2013; Goulet et al. 2017). The exposure and seismic vulnerability models are based on those developed by the GSC as part of the OpenDRR programme. Subsequently, scenario-based earthquake risk assessments are performed by considering finite-fault sources, which are identified from the regional seismic risk assessment and are constrained by new geological and geophysical studies in the WQSZ (Lamontagne et al. 2020; Rimando and Peace 2021). Moreover, sensitivity of regional seismic loss to different characterisations of finite-fault sources and ground motions is investigated. Overall, this study offers new benchmark seismic risk assessments for the WQSZ, which are useful for informing earthquake risk management strategies, including earthquake insurance and disaster relief policies.

2. Quantitative seismic risk model for residential building portfolio in Eastern Canada

2.1. Earthquake catastrophe models

Quantitative risk assessments are essential for disaster risk management and play critical roles in disaster risk financing (Mitchell-Wallace et al. 2017). A general financial risk analysis involves hazard characterisation, exposure database and vulnerability assessment (i.e. risk = hazard × exposure × vulnerability) and requires the incorporation of uncertainties associated with key model components (Foulser-Piggott, Bowman, and Hughes 2020). In this study, two types of complementary earthquake catastrophe models for residential wooden buildings in eastern Canada are developed (note: more than 90% of buildings of the GSC's exposure dataset in Quebec and Ontario are wooden construction). The first model is based on a stochastic event set that characterises the regional seismicity comprehensively and thus facilitates the development of an EP loss curve for a building portfolio of interest (Section 2.1.1). On the other hand, the second model focuses on specific geological faults and develops stochastic finite-fault source models to conduct scenario-based seismic loss estimation (Section 2.1.2). Both catastrophe models are based on the same analytical framework,

consisting of a seismicity model (i.e. stochastic event set [Section 2.2.1] or stochastic finite-fault source model [Section 2.2.2]), a ground motion model (Section 2.3), a building exposure model (Section 2.4) and a seismic vulnerability model (Section 2.5). The details of the key model components are given below. For both types of seismic risk assessments, exposure data and seismic vulnerability functions for wooden residential buildings are prepared as common model components.

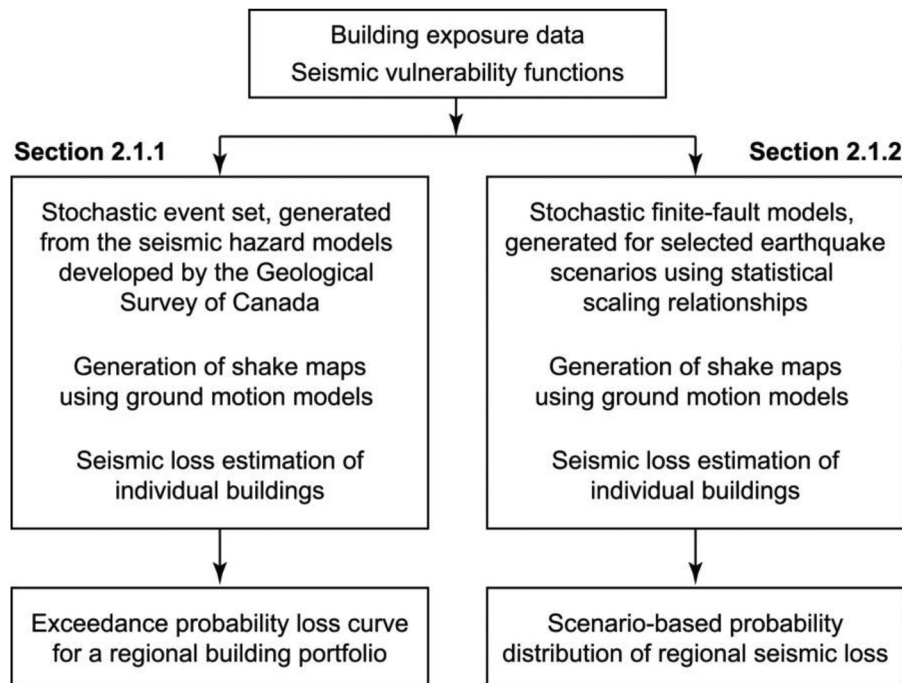### 2.1.1. Regional seismic loss model using a stochastic event set

A seismic loss model for a building portfolio considers a stochastic event set that represents a seismic hazard in a region of interest. The stochastic event set is typically generated based on a seismicity model for probabilistic seismic hazard analysis (Baker, Bradley, and Stafford 2021) and can be used for evaluating an EP curve for a building portfolio of interest (Mitchell-Wallace et al. 2017). The stochastic event set contains information on occurrence time, location, magnitude, and source characteristics, and spans over a long duration. The main computational steps of regional portfolio seismic risk analysis are described below, together with a flowchart shown in Figure 2:

1. A regional stochastic event set is generated using the seismicity models developed by the GSC (Section 2.2.1).

2. For each seismic event in the stochastic set, a suitable ground motion model is selected by considering epistemic uncertainty (Section 2.3), and subsequently, ground motion intensities over a region of interest (i.e. shake map) are simulated using the ground motion model, spatial correlation model and local site condition.

3. For each ground motion value at a building site, an applicable seismic vulnerability model is used to estimate the total loss of a building (Section 2.5). The same calculation is repeated for all buildings.

4. Steps 2 and 3 are then repeated for all stochastic events to calculate seismic losses to individual buildings. Using the event-based seismic loss results for individual buildings, portfolio-level aggregate seismic risk metrics and EP loss curves can be derived and used for financial earthquake risk analysis.

2.1.2. Scenario-based seismic loss model using stochastic finite-fault source models

The second model is developed to evaluate scenario-based portfolio seismic loss for residential wooden buildings in eastern Canada. The earthquake scenario can be selected based on the regional seismic risk assessment via seismic loss disaggregation (Goda and Hong 2009) and is specified in terms of earthquake magnitude and finite-fault source. For a given earthquake scenario, numerous stochastic finite-fault sources can be

Figure 2. Flowchart of regional seismic loss assessments for a building portfolio in eastern Canada using a stochastic event set (Section 2.1.1) and stochastic finite-fault source models (Section 2.1.2).

generated by varying the fault rupture location, geometry and slip distribution (Goda 2017). The key computational steps of the scenario-based earthquake loss estimation method are described below, and its flowchart is also included in Figure 2.

1. A suitable earthquake scenario and its characteristics are defined based on historical events as well as regional earthquake risk results, such as those from Section 2.1.1. An overall fault plane boundary is specified based on geological information that is available for the region. Subsequently, stochastic source modelling is implemented to generate numerous earthquake ruptures with variable fault geometry and earthquake slip distributions (Section 2.2.2). Each finite-fault model represents a possible realised event of the considered scenario.
2. An earthquake shake map is generated for each stochastic source model developed in Step 1 by applying a ground motion model and spatial correlation model (Section 2.3).
3. Seismic vulnerability functions are applied to generate a seismic loss map for the scenario using the ground shaking map simulated in the above step (Section 2.5).
4. Portfolio-level aggregate seismic risk metrics for the earthquake scenario can be derived by repeating Steps 2 and 3 above for all stochastic realisations of potential source models.

2.2. Seismicity models and finite-fault sources for Western Quebec seismic zone

Two types of earthquake source characterisations are carried out for the WQSZ. The seismic source zone-based characterisation is used for generating a stochastic event set (Section 2.1.1), whereas the finite-fault-based characterisation is considered for generating a stochastic source model (Section 2.1.2).

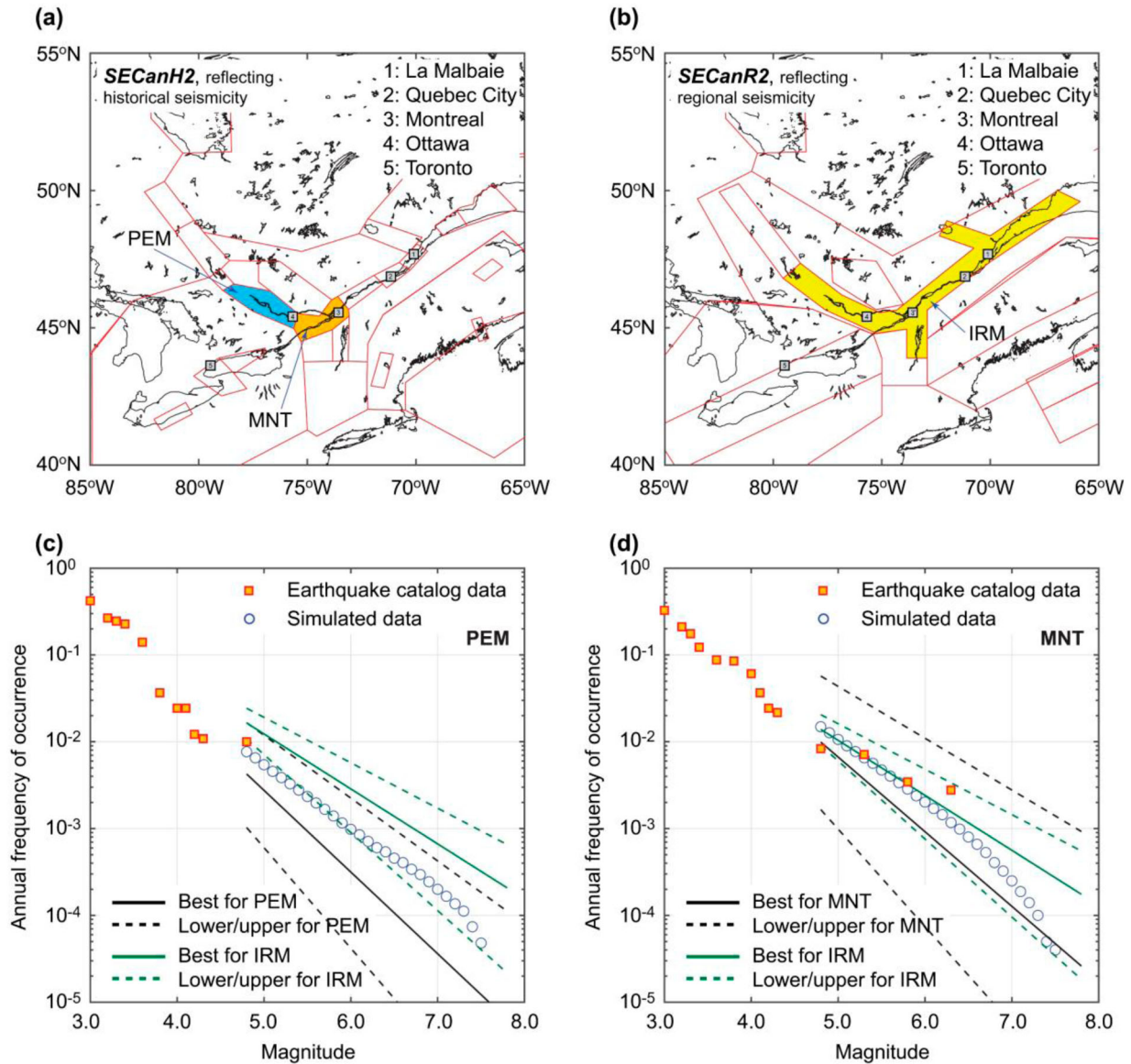### 2.2.1. Historical and regional seismicity models by the geological survey of Canada

The GSC develops national seismic hazard models, which typically consist of seismicity models, ground motion models and logic-tree models for characterising epistemic uncertainty of the model components and parameters. In this study, the 5th generation national seismic hazard model (Halchuk et al. 2014) is adopted, which has been recently updated to the 6th generation model (Kolaj et al. 2020). The major differences of the two generations are attributed to different sets of the ground motion models (Section 2.3), while the

seismicity models are not updated between the 5th and 6th generation seismic hazard models.

Three source zone models for eastern Canada are relevant: *SECanH2*, *SECanHybrid* and *SECanR2*. The *SECanH2* and *SECanR2* source models are shown in Figure 3(a and b), respectively (note: the *SECanHybrid* model is based on the combination of the *SECanH2* and *SECanR2* models). *SECanH2* and *SECanR2* models are areal sources that are characterised based on historical seismicity and regional seismotectonic features, respectively; consequently, the *SECanH2* model consists of smaller (more localised) areal sources compared to the *SECanR2* model (Figure 3). In the GSC's eastern seismic hazard model, logic-tree weights of the source models *SECanH2*, *SECanHybrid* and *SECanR2* reflect the epistemic uncertainty of regional seismicity and are set to 0.4, 0.4 and 0.2, respectively. Within each seismic source zone (i.e. polygons shown in Figure 3), uniform spatial seismicity is considered, together with three logic-tree branches of focal depth (best/lower/upper) having weights of 0.5, 0.25 and 0.25, respectively.

In the 5th generation seismic hazard model, seismicity in each source zone is characterised using the truncated Gutenberg-Richter (G-R) relationship. The minimum magnitude for the hazard calculation is set to 4.8. To capture epistemic uncertainty of source's seismicity, three cases (best/lower/upper) are specified for the *a*-value (N_0) and *b*-value (β) of the G-R relationship with logic-tree weights of 0.68, 0.16 and 0.16, respectively, whereas additional three cases (best/lower/upper) are specified for the maximum magnitude with logic-tree weights of 0.6, 0.3 and 0.1, respectively. Typical maximum magnitudes are 7.8, 7.4 and 8.0 for best, lower and upper cases, respectively. The logic-tree branches are combined independently – thus there are nine cases for the G-R relationship for a given source zone. To illustrate local seismicity within the WQSZ, G-R relationships for the seismic zones PEM and MNT (see Figure 3(a)), where Ottawa and Montreal are located, are compared in Figure 3(c and d) (black solid and broken lines) with historical seismic activity rates based on the earthquake dataset shown in Figure 1 by considering the catalog completeness tables for these sources. In Figure 3(c and d), G-R relationships for the regional seismic source IRM (see Figure 3(b)), which are adjusted for the areas of PEM and MNT, are also included (green solid and broken lines) because these relationships are applicable when the *SECanR2* and *SECanHybrid* models are considered. The uncertainty of the seismicity rates for these two source zones is large.

Using a Monte Carlo-based procedure, a stochastic event set is generated by sampling the occurrence

Figure 3. (a) Historical and (b) regional source zone models for eastern Canada (Halchuk et al. 2014). Comparison of the Gutenberg-Richter relationships for the source zones (c) PEM and (d) MNT in *SECanH2* with the seismic activity rates based on the historical seismic catalog data shown in Figure 1. In (a) and (b), red polygons represent the boundaries of the areal source zone models.

times, locations and magnitudes of earthquakes according to the source zone models and by considering logic-tree weights for epistemic variables. In this study, the duration of the simulated stochastic event set is selected as 500,000 years, noting that all seismic sources are characterised by time-independent Poisson processes. In other words, the simulated stochastic event set can be viewed as 500,000 realisations of 1-year long synthetic earthquake catalog. The centre of the stochastic event set is at 45.529°N and 73.556°W (Montreal) and all events within 1000 km radius are included in the event set. This results in 137,604 events (M > 4.8). The simulated events are shown in Figure 4. Broadly, the spatial distributions of the stochastic events resemble

the observed historical seismicity (Figure 1). To show the general consistency of the observed and modelled seismic activity rates, the simulated seismicity rates for PEM and MNT (blue circles) are included in Figure 3 (c and d), respectively.

2.2.2. Geological fault data and stochastic source models

The Saint Lawrence region is an extensive, intraplate continental region characterised by spatial clustering of weak to moderate recent seismicity which likely results from the reactivation under the present-day tectonic stress field of inherited structures (Mazzotti and Townend 2010; Rimando and Peace 2021). Major
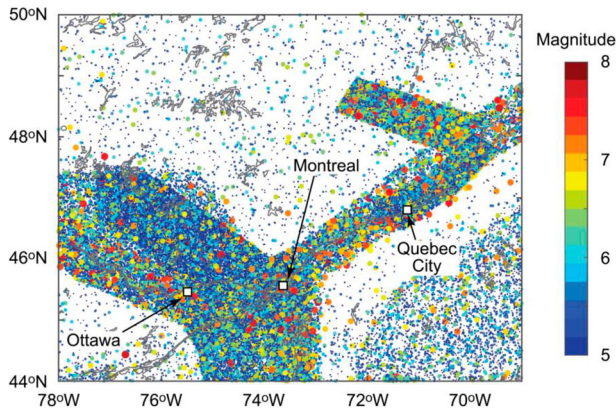
Figure 4. 500,000-year stochastic event set for eastern Canada generated from the 5th generation seismic hazard model for eastern Canada.

tectonic features include grabens and half-grabens that belong to the Saint Lawrence rift system, such as the Ottawa-Bonnechere and Timiskaming grabens, that are composed primarily of NW- and NE-striking, steeply dipping valley-forming faults. In the absence of a map of active faults, a good first step for the finite-fault source characterisation is to determine the potential of pre-existing faults to be reactivated under the current stress field. Recently, using slip tendency analysis, Rimando and Peace (2021) conducted 3D numerical stress simulations to explore the preferred spatial distribution and trends, and predicted sense of slip of reactivated pre-existing structures in the WQSZ under the current tectonic stress field. Slip tendency is the ratio of the shear stress to normal stress on a fault plane and has been used in different tectonic settings worldwide to characterise the relative likelihood of populations of faults to slip under current or past stress fields (Morris, Ferrill, and Henderson 1996; Peace et al. 2018). This method can highlight structures and regions that are susceptible to Quaternary seismic activity.

Recently, Lamontagne et al. (2020) compiled a database of geological lineaments including faults in the WQSZ. The locations of these potentially active faults are shown in Figure 5(a). Considering that these potentially active faults are capable of hosting major earthquakes (Rimando and Peace 2021), we focus on two possible fault rupture scenarios near Ottawa and Montreal. For Ottawa, the Hazeldean fault, denoted by WQ-PEM in Figure 5(a), is considered as a critical source as it passes south of Ottawa. The length and width of the fault plane are set to 78 and 30 km, respectively. The fault length is determined by connecting the first and last points of the geological lineaments of the fault, and the maximum magnitude and fault width

are estimated using empirical earthquake source scaling relationships by Thingbaijam, Mai, and Goda (2017). Assuming that a full rupture of the defined fault plane is possible, M7 events can be hosted. For Montreal, the Milles-Iles fault, denoted by WQ-MNT in Figure 5 (a), is considered as a critical seismic source that can cause severe seismic damage in Greater Montreal. The length and width of the fault plane are set to 30 and 22 km, respectively. The source can cause earthquakes up to M6.5 (based on the fault length). For both finite-fault sources, the strike angle of the fault source is based on the geometry specified in the fault database by Lamontagne et al. (2020), whereas the dip angle (= 60°) is adapted from simulations conducted by Rimando and Peace (2021). The top depth of the fault plane is assumed to be 5 km; with the assumed fault widths and the dip angle for the two finite-fault sources, the focal depth of the events is typically distributed between 10 and 20 km, when the empirical rules suggested by Mai, Spudich, and Boatwright (2005) for the hypocentre locations are applied.

For stochastic source modelling, the finite-fault sources for WQ-PEM and WQ-MNT are discretized into multiple sub-faults (2 km by 2 km; see Figure 5(b and c)). Then, a stochastic source model is generated by sampling eight source parameters, i.e. fault length, fault width, mean slip, maximum slip, Box–Cox parameter, along-strike correlation length, along-dip correlation length, and Hurst number from the statistical scaling relationships (Goda 2017), and by synthesising a heterogenous earthquake distribution based on the simulated source parameters (Mai and Beroza 2002). When the length and width are smaller than the overall fault plane of the considered scenario (as indicated in the right-hand side of Figure 5(a)), the simulated finite-fault source is floated within the target finite-fault plane. Further details of the stochastic source generation can be found in Goda (2017).

In this study, three scenario magnitudes (M6.0, M6.5 and M7.0) are considered for WQ-PEM, whereas two scenario magnitudes (M6.0 and M6.5) are considered for WQ-MNT. Each magnitude scenario is defined with a range of plus and minus 0.1 magnitude unit with respect to the representative value. For instance, the M6.0 scenario has magnitudes between M5.9 and M6.1. A larger magnitude scenario of M7.0 is considered for WQ-PEM because it can accommodate M7.0 events based on its fault length, while such large events are unlikely for WQ-MNT from empirical viewpoints of earthquake scaling relationships. Moreover, the considered scenario magnitudes for these two sources are smaller than the maximum magnitudes specified for the areal sources by the GSC, such as
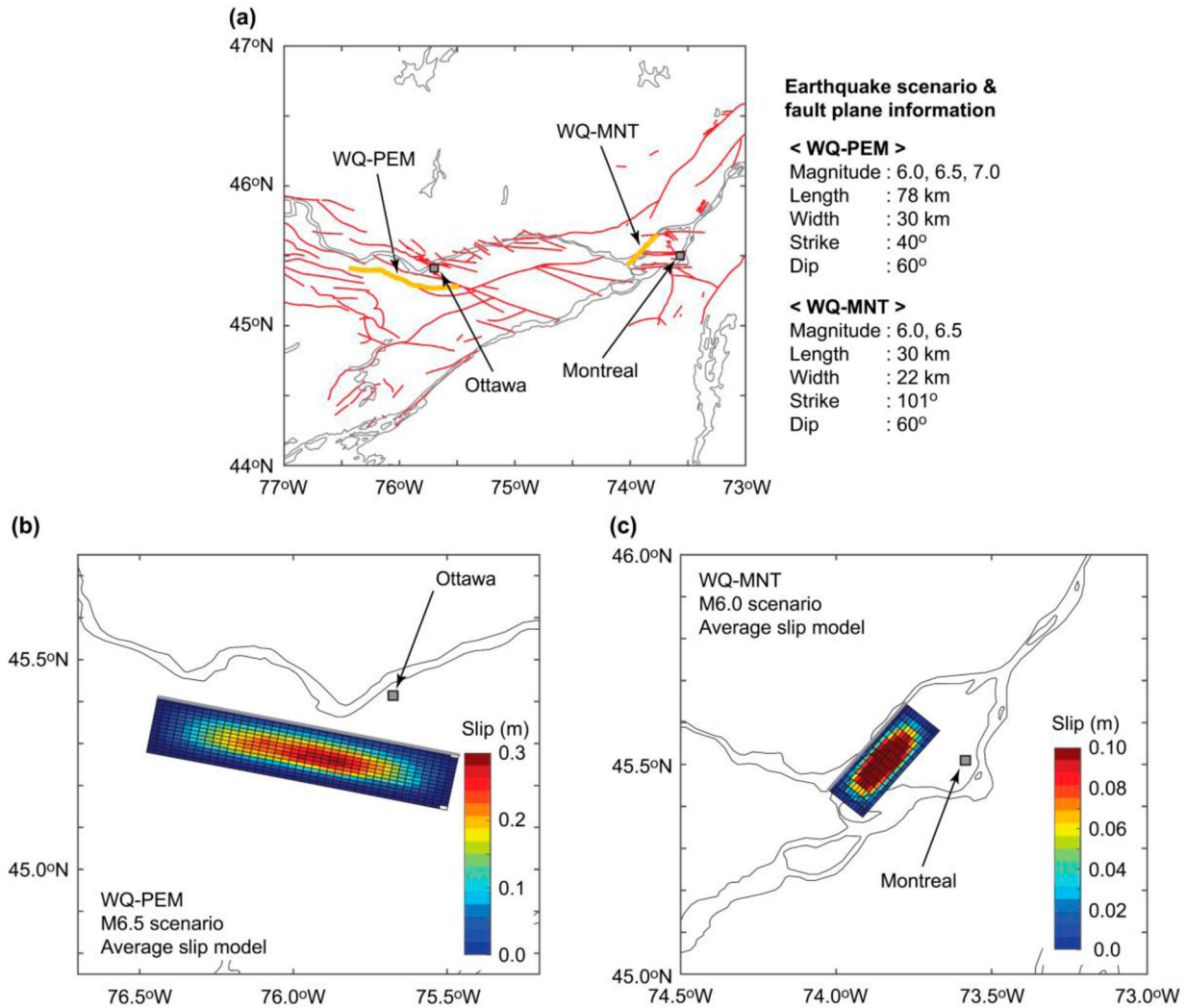
Figure 5. (a) Geological lineaments in the Montreal-Ottawa region based on Lamontagne et al. (2020), (b) average slip distribution for the M6.5 WQ-PEM scenario and (c) average slip distribution for the M6.0 WQ-MNT scenario.

PEM and MNT shown in Figure 3 (typically in the range of M7.4 to M8.0). For a given scenario magnitude, 1000 realisations of stochastic finite-fault sources are generated and are used for scenario-based seismic loss estimation of residential buildings (Section 2.1.2). Figure 5(b and c) show the average slip distributions based on the 1000 realisations of stochastic finite-fault sources for the M6.5 WQ-PEM scenario and the M6.0 WQ-MNT scenario, respectively. It is noted that the maximum values of the average slip distributions shown in Figure 5(b and c) are smaller than the maximum values of the simulated stochastic slip distributions. This is because for most of the earthquake scenarios considered, the fault dimensions of the stochastic source models are smaller than the target finite-fault planes and the simulated slip distributions float within the target finite-fault planes. For instance, based on the adopted scaling relationships, the average slip values of the M6.5 WQ-PEM scenario and the M6.0 WQ-

MNT scenario are approximately 0.5 and 0.25 m, respectively, whereas the maximum slip values of the M6.5 WQ-PEM scenario and the M6.0 WQ-MNT scenario are approximately 1.8 and 0.9 m, respectively.

2.3. Ground motion models for Eastern Canada

In this study, two sets of ground motion models for eastern Canada are implemented. The first set is for the 5th generation 2015 GSC model (Halchuk et al. 2014), whereas the second set is for the 6th generation 2020 GSC model (Kolaj et al. 2020). The ground motion models for the 2015 GSC model are based on Atkinson and Adams (2013) and consist of three median prediction equations (best/lower/upper) with logic-tree weights of 0.5, 0.2 and 0.3, respectively. The ground motion models for the 2020 GSC model are the so-called NGA-East model for stable continental regions (Goulet et al. 2017), consisting of 13 logic-tree branches

(note: weights are variable for different earthquake scenarios). An important advantage of the NGA-East model for conducting scenario-based seismic loss estimation with detailed source models is that its distance measure is the closest distance to rupture plane, which reflects the finite dimension of the earthquake source, instead of a simplistic hypocentral distance. On the other hand, a major disadvantage of using the NGA-East model is that the model implementation requires a suitable site response model, because the NGA-East model suite is only developed for a very hard rock site condition of average shear wave velocity in the uppermost 30 m (V_{S30}) equal to 3000 m/s. To resolve the latter issue, Kolaj et al. (2020) implemented an applicable site amplification model for the NGA-East model. In the 2020 GSC seismic hazard model, two suites of the ground motion models by Atkinson and Adams (2013) and by Goulet et al. (2017) were considered with equal weights of 0.5. As part of the 2020 GSC seismic hazard model, Kolaj et al. (2020) provided tabulated values of the median ground motion models for a wide range of local site conditions represented by different V_{S30} values. To follow GSC's calculation procedure closely, tabulated versions of the ground motion models are implemented in this study, and ground motions for unspecified values of earthquake scenarios in terms of magnitude, distance and V_{S30} are obtained by interpolation. It is important to note that the site effects that are considered in this study are simplistic; no nonlinear site effects are accounted for and V_{S30} values are crude estimates of subsurface ground conditions based on topographical slopes. Future studies should investigate these effects on ground motions as well as seismic losses.

To illustrate the magnitude scaling and distance attenuation of the median ground motions for the Atkinson–Adams model and the Goulet et al. model, as implemented in Kolaj et al. (2020), the two suites of the ground motion models are shown in Figure 6 for two magnitude values (M6.0 and M7.0). In the figure, spectral acceleration (SA) at 0.3 s is selected because it is a representative seismic intensity parameter for seismic vulnerability functions of residential wooden buildings (Section 2.5). Moreover, three or thirteen median equations of the logic-tree branches are shown with black lines, whereas the total prediction interval, which includes the effects due to uncertain median models and those due to aleatoric prediction errors, is shown with red lines with + symbols. Generally speaking, the Goulet et al. model predicts higher median ground motion values, especially at distances around 50–150 km and captures a wider range of epistemic uncertainty associated with the median ground motions, compared with the Atkinson–Adams model.

The comparison of the ground motion model plots clearly highlights the extent of epistemic uncertainty incorporated in the two ground motion model suites (i.e. variations of black lines). This increased variability of the ground motion models is the main driver of the increase of the final seismic hazard values in the 6th generation seismic hazard model for eastern Canada.

The effects of aleatory variability of ground motion parameters (i.e. sigma) are considered by simulating normally distributed error terms (in logarithmic scale). Empirically, it has been observed that the intra-event residuals of the ground motion models are spatially correlated at closer locations than at more distant locations. This aspect is incorporated by simulating shake maps probabilistically using the intra-event spatial correlation model of Goda and Atkinson (2010). To capture local site conditions at the building locations, V_{S30} is adopted as a site parameter. Due to the lack of direct measurements of this site parameter across Canada uniformly, surrogate estimates of V_{S30} based on topographical slopes (Wald and Allen 2007; Heath et al. 2020) are considered.

In simulating ground motion values in the WQSZ region, grids are defined at 0.02-degree resolution (approximately 2-km grids) and ground motion intensities are evaluated at this resolution. Note that the grid resolution for the V_{S30} data is approximately at 1-km grids, and the closest V_{S30} data are assigned to the ground motion simulation grids. The adopted ground motion grids are selected based on two considerations. A main reason is the computational cost associated with simulations of spatially correlated ground motion fields (i.e. probabilistic shake map). The other reason is that the spatial correlation model is not calibrated with abundant ground motion data pairs with separation distances less than 1 km (Goda and Atkinson 2010). Once ground motions are simulated regionally, the corresponding ground motion values at the building sites are obtained by interpolation (Section 2.4).

2.4. Building exposure model for Eastern Canada

The regional seismic loss models developed in this study adopt a nationwide building exposure database developed by the GSC (note: the data were provided in 2020). The building exposure model contains information on: building locations, building numbers (per location with the same typology), building asset values for structural, non-structural and contents elements, occupants' numbers in day, night and transit situations, land use, occupancy (agricultural/civic/commercial/industrial/residential), building material (concrete/
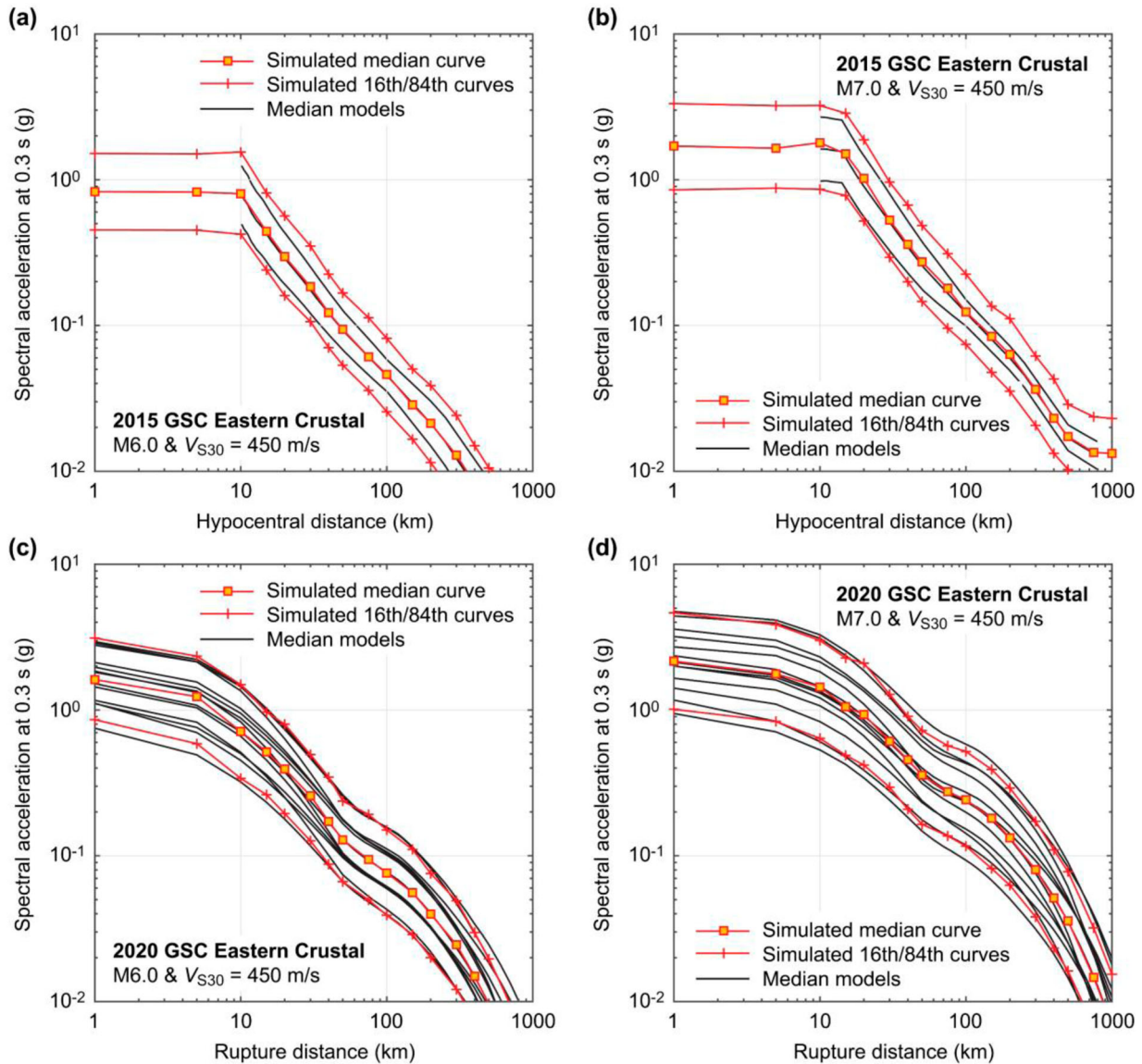
Figure 6. Ground motion models for shallow crustal earthquakes for eastern Canada: (a) 2015 GSC model – M6.0, (b) 2015 GSC model – M7.0, (c) 2020 GSC model – M6.0 and (d) 2020 GSC model – M7.0.

manufactured/precast/reinforced masonry/steel/unreinforced masonry/wood) and HAZUS-based typology in terms of building class and earthquake design code level as explained by Ulmi et al. (2014).

The data entry is based on the combined building typology, which differentiates building occupancy types and earthquake-related building types. This essentially determines the resolution of the exposure database. For most cases, the building number per specified type is less than 10, while for a large residential complex, the building number can be over 100. The building occupancy class is related to building values and occupant numbers (and thus affect the seismic loss estimation results). On the other hand, the building material and the HAZUS-based building classes are related to seismic vulnerability functions (Section 2.5).

Most buildings in Canada are timber constructions (92%), and timber buildings consist of 53% of the total building asset value. For wooden buildings, the overall proportions of structural, non-structural and contents elements with respect to the total asset values are 17%, 52% and 31%, respectively. In this study, residential wooden buildings, which are specified as *W1* or *W2* HAZUS building typology, are considered for portfolio seismic risk assessments. *W1* corresponds to a wooden light frame (typically 1–2 stories), whereas *W2* corresponds to a larger wooden frame (typically with 3–6 stories). The spatial distributions of these buildings are shown in Figure 7(a), whereas V_{S30} data for the building locations are shown in Figure 7(b). It is noted that the locations shown in Figure 7 are based on the 0.02-degree grids that are used for
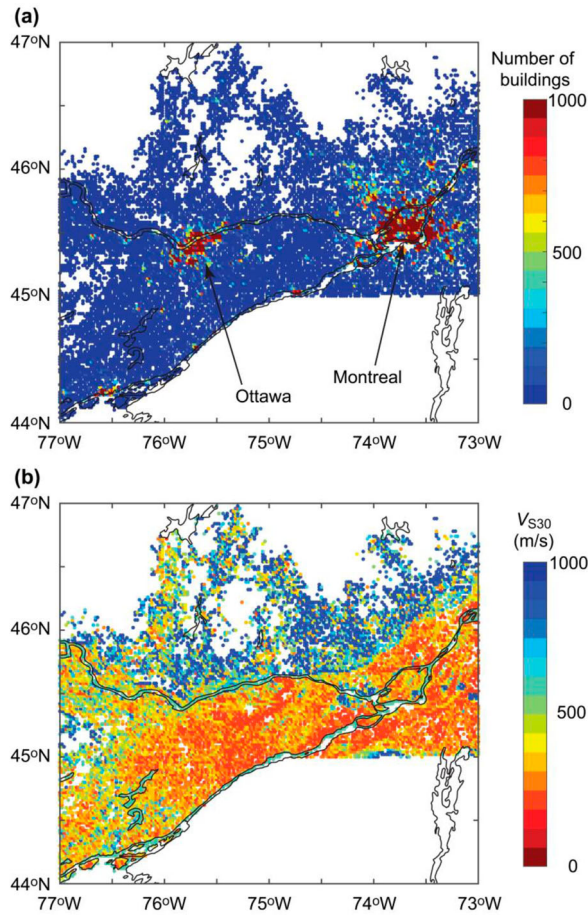
Figure 7. (a) Distribution of residential wooden buildings and (b) average shear-wave velocity data for the Western Quebec seismic zone.

simulating ground motion intensity values. The V_{S30} data in the WQSZ range between 190 and 900 m/s. The building distributions are concentrated near Ottawa and Montreal, and site conditions in the Saint Lawrence region are generally soft (site class D, which corresponds to sites with V_{S30} between 180 and 360

m/s). In total, 2,128,398 houses are included in the building portfolio and are distributed over 33,449 sites within the region shown in Figure 7. The total asset value of the portfolio is C$1430.9 billion.

2.5. Seismic vulnerability models for Eastern Canada

Seismic vulnerability models quantify the degree of seismic loss to a building as a function of the seismic intensity parameter. The seismic vulnerability functions for residential wooden buildings in Canada are obtained from the GSC. The seismic vulnerability functions are provided by expressing a mean loss ratio as a function of SA at a vibration period, which is applicable to a relevant building system, and are defined in conjunction with the building exposure database. As mentioned in Section 2.4, a building system and its total asset value are represented by structural, non-structural and contents elements. For each building element, an applicable mean seismic vulnerability function is specified. Therefore, for a given seismic excitation, three loss ratios can be obtained from the mean vulnerability functions for the three elements, and then the weighted average can be computed to represent the total building loss in monetary terms. Figure 8(a–c) show mean seismic vulnerability functions for structural, non-structural and contents elements, respectively. The input ground motion parameter of the seismic vulnerability functions is SA at 0.3 s. The ground motion intensity measure (i.e. SA at 0.3 s) for the seismic vulnerability functions was selected by the GSC, noting that the chosen parameter is consistent with previous studies that investigated relationships between ground motion intensity measures and seismic damage severities (Wesson et al. 2004; Goda 2019). For eastern Canada, there are 33 different building typologies, consisting of a
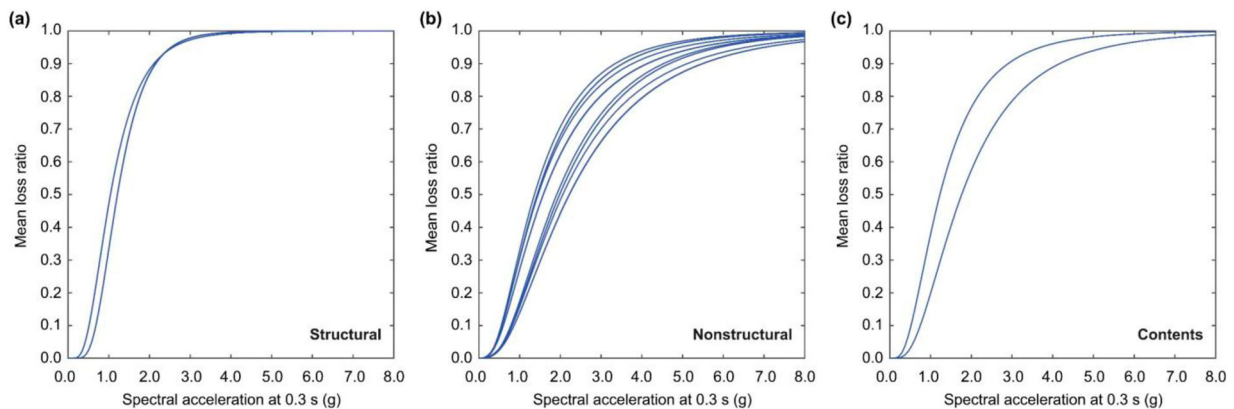
Figure 8. Mean vulnerability functions for (a) structural, (b) non-structural and (c) contents elements for residential buildings in Quebec and Ontario.
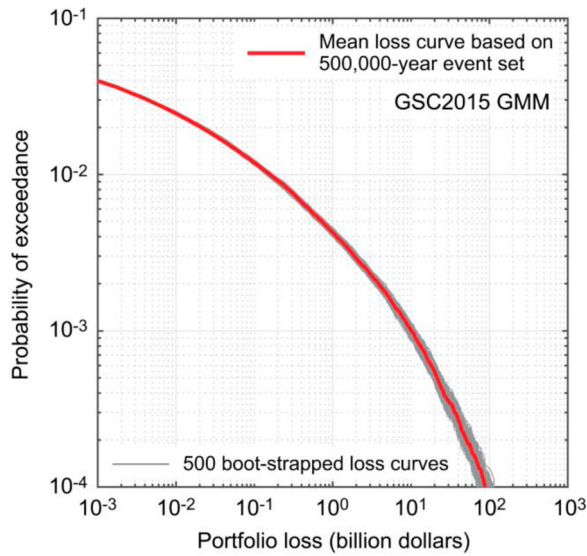
Figure 9. Exceedance probability loss curve for the wooden building portfolio in the Western Quebec seismic region.

combination of two building types (*W1* or *W2*), nine occupancy types (*RES1*, *RES3A/B/C/D/E/F*, *RES4* or *RES6*), and two seismic design levels (*PC* [pre-code] or *LC* [low code]) (note: some combinations of building, occupancy and design types do not exist). The structural vulnerability functions are mainly affected by two seismic design levels (Figure 8(a)), and none of the wooden buildings in eastern Canada are designated with modern seismic design codes (Hobbs, Journeay, and LeSueur 2021). The non-structural vulnerability functions are affected by both building and occupancy types (Figure 8 (b)), whereas the contents vulnerability functions mainly depend on the building type.

The GSC's seismic vulnerability functions only reflect the mean loss ratios in terms of ground motion hazard experienced. This representation is simplistic as variability of the earthquake damage and loss assessment is usually significant. To consider this neglected uncertainty, the seismic loss of an individual building is treated as a random variable, characterised by the lognormal distribution with the mean loss predicted by the vulnerability functions for a given SA at 0.3 s (Figure 8) and the coefficient of variation equal to 0.6. This value of the coefficient of variation reflects the uncertainty associated with the damage extent of an individual building for a given seismic intensity as well as the uncertainty of the building reconstruction cost. More specifically, the coefficient of variation of 0.6 is selected based on the empirical insurance loss model developed by Wesson et al. (2004) using the insurance claim data for single-family wooden households in California after the 1994 Northridge earthquake. The earthquake insurance claim data were based on 80,516 claims

from 266 ZIP codes with a total claim amount of US$ 3.4 billion. The claim data and developed empirical insurance loss models by Wesson et al. (2004) can be viewed as the most realistic empirical reference for wooden houses in North America. In generating seismic losses for portfolio seismic risk assessments (Section 3), values for different buildings are not considered to be correlated. However, because several buildings at the same location are treated as one entity in the exposure data, seismic vulnerability assessments are partially correlated.

3. Seismic loss estimation for residential wooden buildings in the Western Quebec seismic zone

Regional seismic loss estimation of residential wooden buildings is carried out for the WQSZ. Firstly, in Section 3.1, the stochastic event set that is generated from the GSC's seismic hazard model for eastern Canada (Section 2.2.1) is employed to obtain the EP loss curve for the building portfolio (Section 2.4) and critical seismic loss events are identified. Subsequently, in Section 3.2, two finite-fault sources that could affect two major urban areas of the WQSZ, i.e. Ottawa and Montreal, are focused upon to perform scenario-based seismic loss estimation using stochastic finite-fault source models (Section 2.2.2). By associating major loss-generating events with potentially active geological faults in the WQSZ, more detailed seismic risk assessments can be conducted. Sensitivity of the scenario-based regional seismic loss estimation to varied fault source characteristics, scenario magnitudes and alternative ground motion models is investigated in this section.

3.1. Exceedance probability loss curves for the Western Quebec seismic zone

Using the stochastic event set that spans over 500,000 years (Figure 4), portfolio seismic risk assessments for residential wooden buildings are carried out. Using 500,000 samples of the annual maximum portfolio seismic loss, Figure 9 shows an EP loss curve for the wooden building portfolio in the WQSZ. The ground motion model used is the GSC2015 model (Figures 6(a and b)). This model is compatible with the point-source representation of seismic events in eastern Canada. In the figure, 500 bootstrapped exceedandance probability curves are also included to demonstrate the confidence interval of the mean seismic loss curve by resampling 500,000 annual maximum portfolio seismic losses with replacement. As expected, the confidence interval tends to be wider as the probability of exceedance
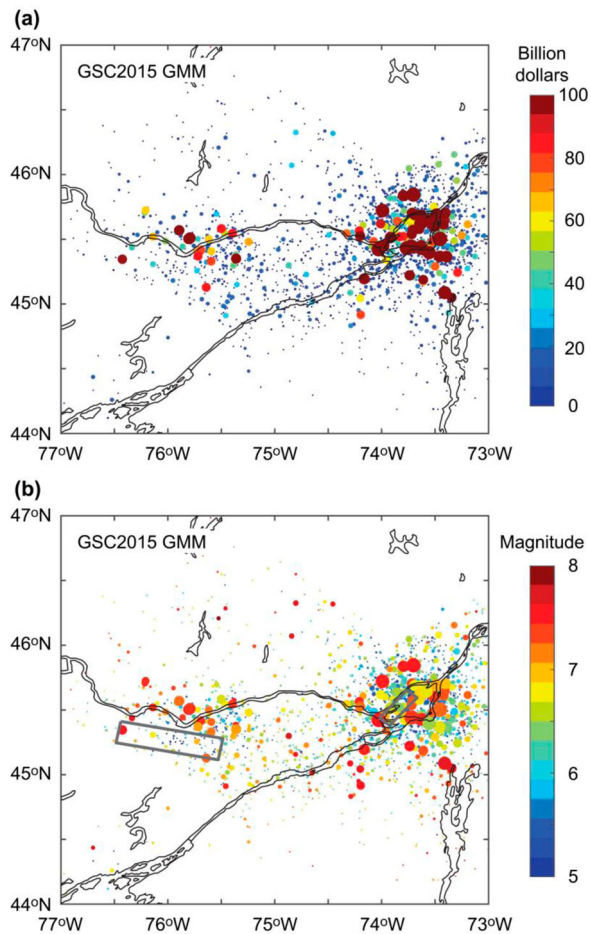
Figure 10. Spatial distribution of major seismic loss events that cause more than C$1 billion portfolio loss with the size and colour of the circles representing (a) portfolio seismic loss and (b) earthquake magnitude.

becomes smaller, but with the sample size of 500,000, the mean EP curve is relatively well constrained up to 10^{-4} probability level. It is noted that the confidence interval shown in Figure 9 only reflects the standard error of the mean curve, and does not represent other fractile curves in terms of epistemic uncertainty of the seismic hazard model considered by the GSC.

The regional portfolio seismic loss for residential wooden buildings in the WQSZ increases rapidly, for instance, from C$0.16 billion at 10^{-2} probability level, C$10.1 billion at 10^{-3} probability level, to C$87.4 billion at 10^{-4} probability level. From practical viewpoints of financial seismic risk management (return periods of 500–1000 years), up to C$10 billion loss events can be relevant for the residential sector. These losses do not include financial risks to other types of buildings and commercial/public sector buildings nor those caused by landslides and fires following earthquakes. It is also important to recognise that although it is rare, there is a chance that a catastrophic earthquake loss, exceeding C$10 billion loss, could be
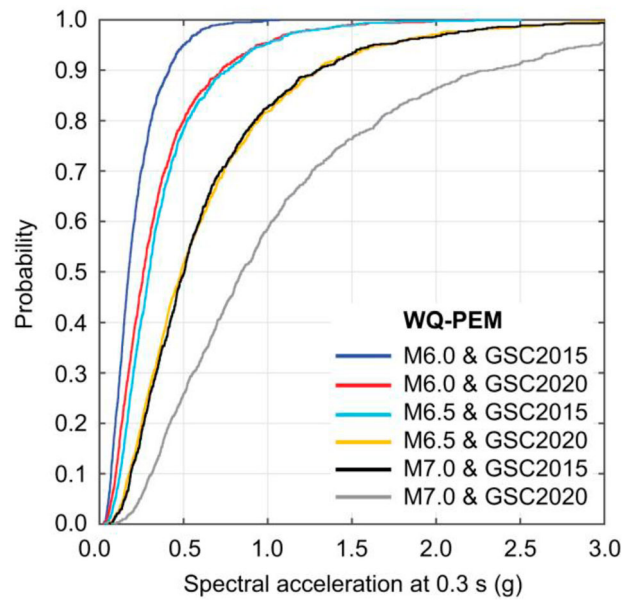

Figure 11. Conditional probability distributions of spectral acceleration at 0.3 s at a site in Ottawa for the WQ-PEM source by considering three scenario magnitudes (M6.0, M6.5 and M7.0) and two ground motion models (GSC2015 and GSC2020).

generated. Note also that this low probability of such a devastating seismic loss event is attributed to the low occurrence probability of moderate-to-large earthquakes in the WQSZ. For instance, the magnitude-recurrence relationship for the source zone MNT (Figure 3(d)) indicates that the chance of having a M6 + event within the zone is in the order of 0.01–0.001. However, when such
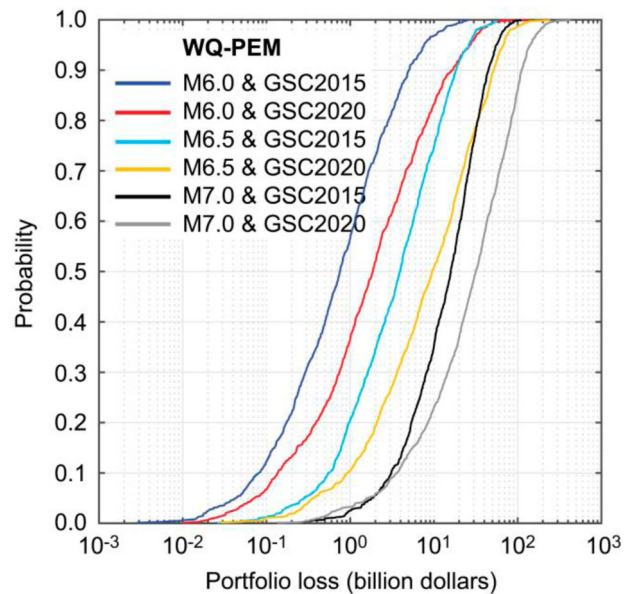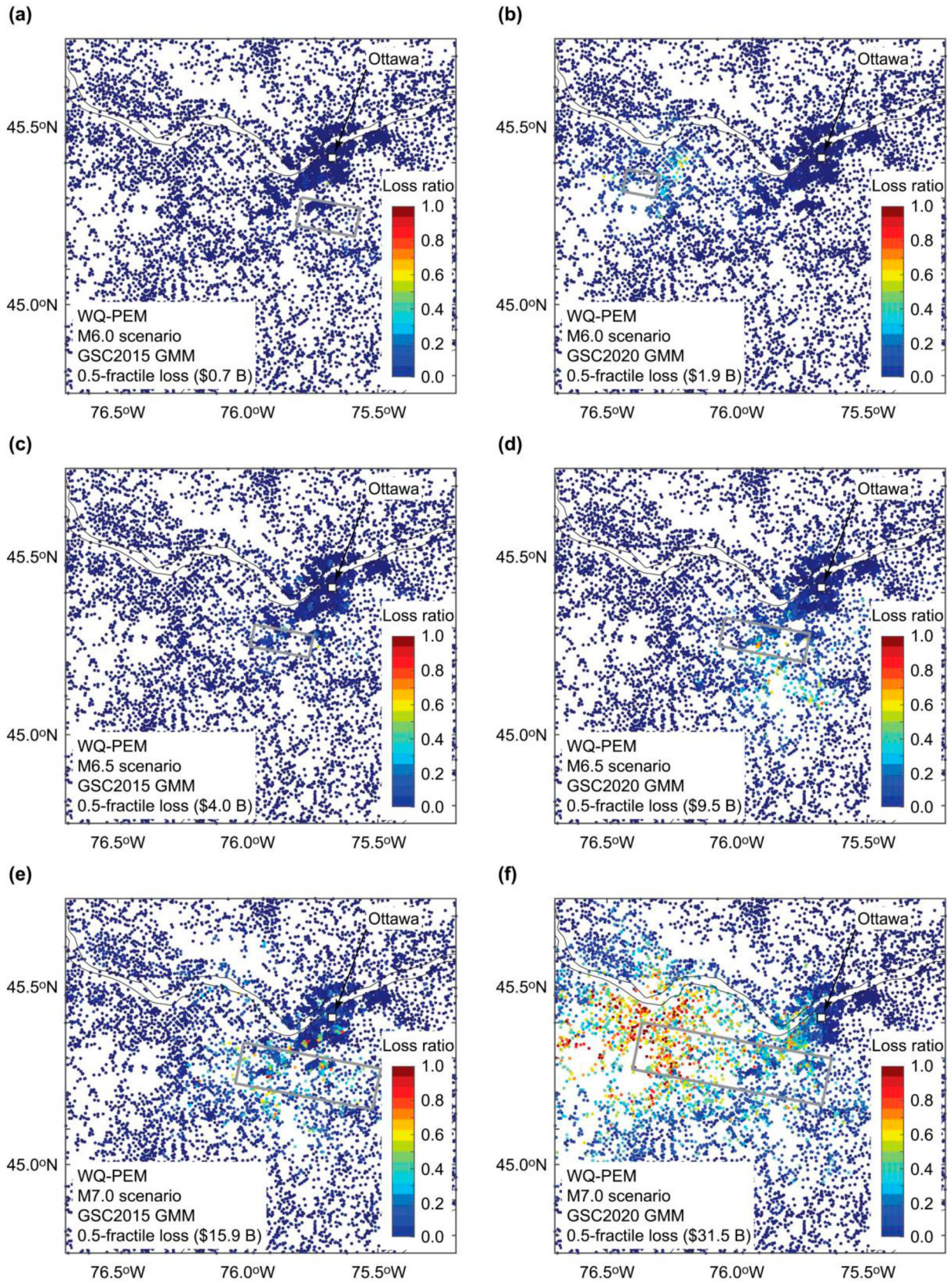

Figure 12. Conditional probability distributions of scenario-based portfolio seismic loss for the WQ-PEM source by considering three scenario magnitudes (M6.0, M6.5 and M7.0) and two ground motion models (GSC2015 and GSC2020).
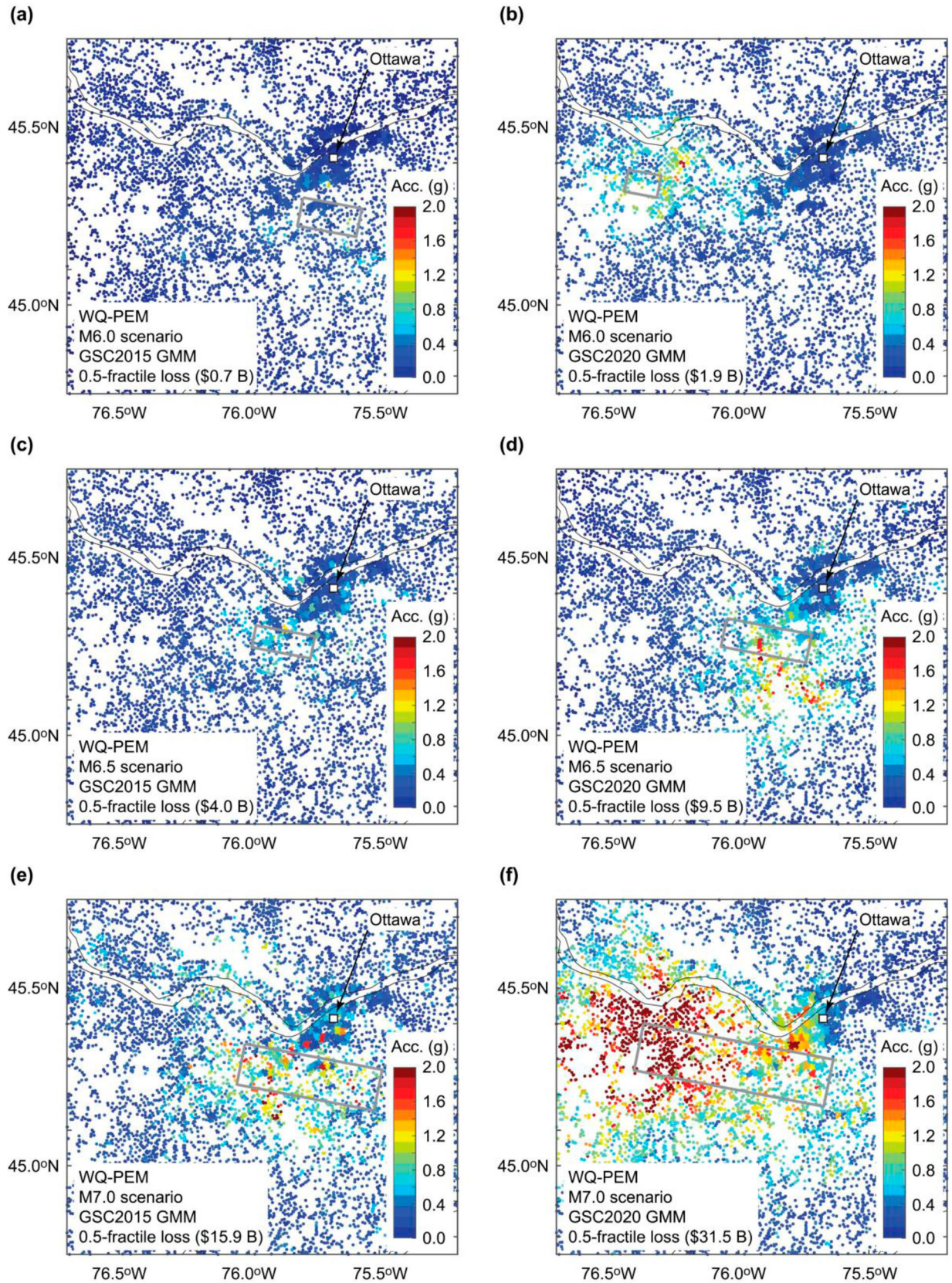
Figure 13. SA at 0.3 s shake maps for the 0.5-fractile (median) seismic loss scenarios for the WQ-PEM source by considering three scenario magnitudes (M6.0 [a,b], M6.5 [c,d] and M7.0 [e,f]) and two ground motion models (GSC2015 [a,c,e] and GSC2020 [b,d,f]). The grey rectangles are the fault plane boundaries of the stochastic source models.

Figure 14. Seismic loss ratio maps for the 0.5-fractile (median) seismic loss scenarios for the WQ-PEM source by considering three scenario magnitudes (M6.0 [a,b], M6.5 [c,d] and M7.0 [e,f]) and two ground motion models (GSC2015 [a,c,e] and GSC2020 [b,d,f]). The grey rectangles are the fault plane boundaries of the stochastic source models.
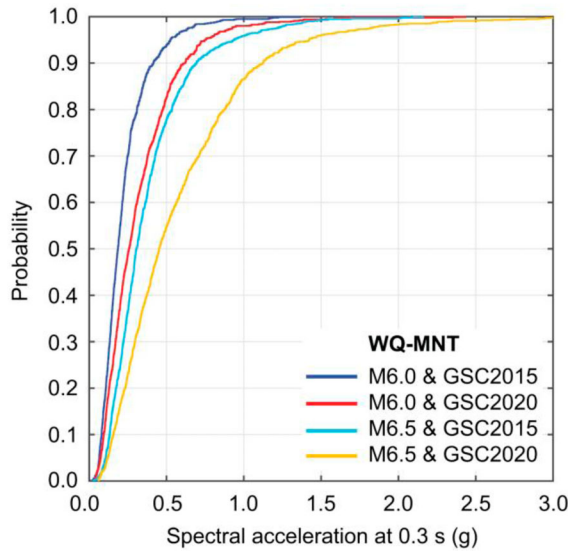
Figure 15. Conditional probability distributions of spectral acceleration at 0.3 s at a site in Montreal for the WQ-MNT source by considering two scenario magnitudes (M6.0 and M6.5) and two ground motion models (GSC2015 and GSC2020).

an event occurs, the seismic loss could be significant, especially at the portfolio perspective because of high concentration of residential wooden buildings near the major urban areas (Figure 7(a)). This heavy right tail risk, although occurring outside of the typical financial/insurance risk management (e.g. return periods between 100 and 1000 years), is an important concern from regional seismic risk emergencies. In this regard, it is important to conduct scenario-based seismic risk assessments for the region because this kind of investigations allows to answer what if type question more directly, and this is the motivation of this study to conduct both types of regional seismic loss estimation.

The portfolio seismic loss estimation based on the stochastic event set produces additional useful results. For example, all major seismic events that cause portfolio seismic loss greater than a threshold value can be identified and their event as well as spatial characteristics can be examined in detail. Figure 10(a and b) show the spatial distributions of major seismic loss events exceeding C\$1 billion in terms of aggregate loss value and earthquake magnitude, respectively. There are 2127 events for such a loss threshold value (i.e. 0.0043 events per year); in other words, on average, a C\$1 billion loss event occurs every 235 years. Figure 10 (a) clearly shows that major loss events occur in the vicinity of Montreal and Ottawa, noting that more risks are associated with Montreal than Ottawa due to greater exposure (Figure 7(a)). Figure 10(b) shows the major loss events in terms of earthquake magnitude. In this figure, the fault planes for the WQ-PEM and WQ-MNT finite-fault sources (Figure 5(b and c)) are

included with grey rectangles. There are several major loss events that fall within the boundaries of the WQ-PEM and WQ-MNT sources, and their magnitudes are in the range between M6 and M7 (light blue to orange colours). Therefore, the two finite-fault sources, which are related to known geological features according to Lamontagne et al. (2020), can be regarded to be possible scenarios for regional seismic risk assessments, as investigated in Section 3.2.

3.2 Scenario-based seismic loss maps for the Western Quebec seismic zone

3.2.1 Critical scenarios near Ottawa

The scenario-based portfolio seismic loss estimation is conducted by considering three sets of 1000 stochastic source models that have different magnitude values, i.e. M6.0, M6.5 and M7.0 scenarios (note: for each scenario, plus and minus 0.1 magnitude range is considered). First, to illustrate the ranges of ground motion intensities from the considered scenarios at a site in Ottawa, conditional probability distributions of SA at 0.3 s are shown in Figure 11. The closest rupture distance from the Ottawa site to the fault source plane is approximately 15 km (Figure 5(b)). Two ground motion models, i.e. GSC2015 and GSC2020, are considered for each scenario. Each distribution is represented by 1000 data points of SA at 0.3 s and captures the variability of the ground motion intensity due to uncertain fault geometry and position within the finite-fault plane. It is
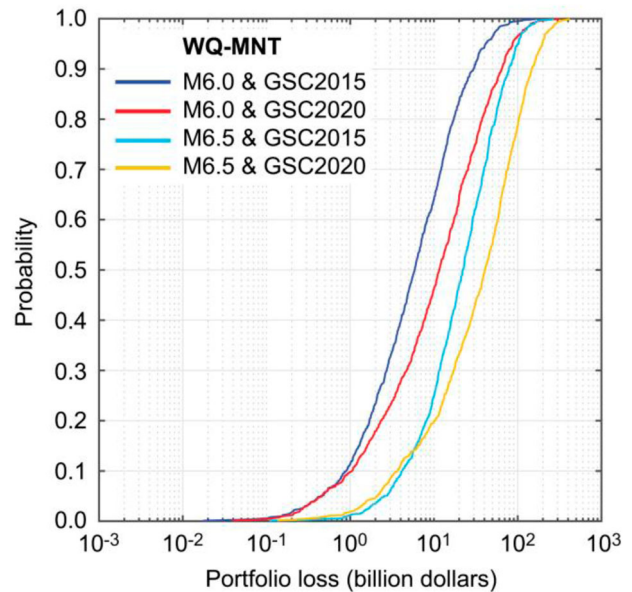

Figure 16. Conditional probability distributions of scenario-based portfolio seismic loss for the WQ-MNT source by considering two scenario magnitudes (M6.0 and M6.5) and two ground motion models (GSC2015 and GSC2020).

noteworthy that since the finite fault sources are directly represented in the stochastic source modelling, ground motion models that are applicable to the finite-fault sources, such as GSC2020, are suitable. Figure 11 shows that with the increase in earthquake magnitude, ground motions become greater (i.e. translational shift of the distribution towards the right-hand side) and the use of the GSC2020 models leads to significant increase of the regional seismic loss compared to the GSC2015 models (Figure 6). The latter effects can be attributed to the greater variability of the predicted ground motion values (i.e. wider ranges of the 16th and 84th curves) and the more gradual distance attenuation of the GSC2020 model than the GSC2015 model.

Figure 12 shows the conditional probability distributions of scenario-based portfolio seismic loss for the WQ-PEM source (Figure 5(b)) by considering the three scenario magnitudes and two ground motion models. The same observations regarding the effects of earthquake magnitude and ground motion model as made

in Figure 11 are applicable to Figure 12. Note that for M6 + events, the differences of the predicted ground motion values at distances less than 50 km are more influential because in these distance ranges, ground motion values can be sufficiently large to cause nonnegligible seismic damage (as can be inspected from Figure 8). Overall, Figure 12 demonstrates the sensitivity of the regional seismic loss to fault-source geometry and position, earthquake magnitude and ground motion model.

It is insightful to investigate how various major events cause ground motion intensities as well as seismic losses across the region. For this purpose, Figure 13 shows scenario-based shake maps (note: these maps are not deterministic, but probabilistic) for the WQ-PEM source by considering the three scenario magnitudes and two ground motion models. For each case, the 0.5 fractile scenario is adopted as representative (i.e. a stochastic source model that corresponds to 501st of regional seismic loss when it is sorted in an ascending order). It can be observed that with the increase in earthquake magnitude,
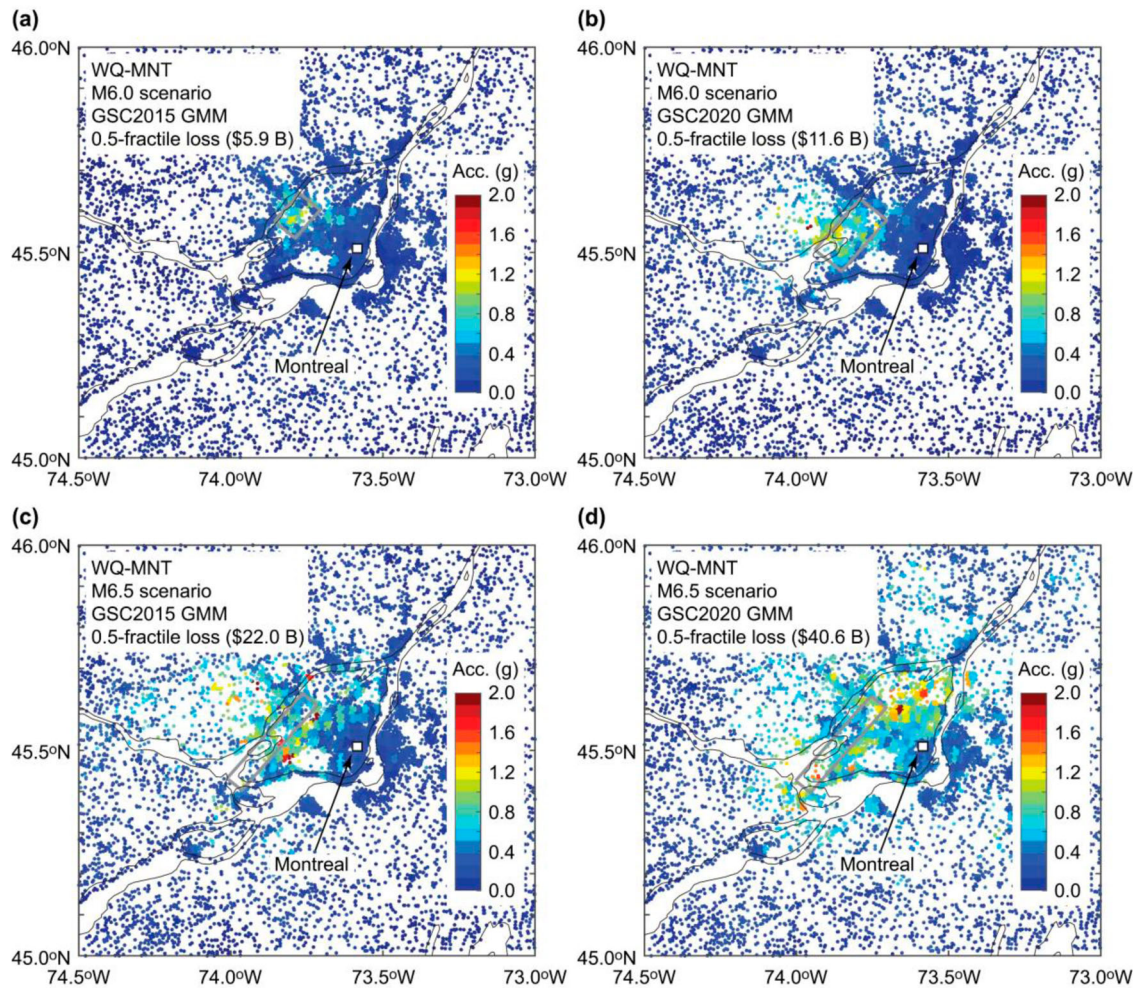
Figure 17. SA at 0.3 s shake maps for the 0.5-fractile (median) seismic loss scenarios for the WQ-MNT source by considering two scenario magnitudes (M6.0 [a,b] and M6.5 [c,d]) and two ground motion models (GSC2015 [a,c] and GSC2020 [b,d]). The grey rectangles are the fault plane boundaries of the stochastic source models.
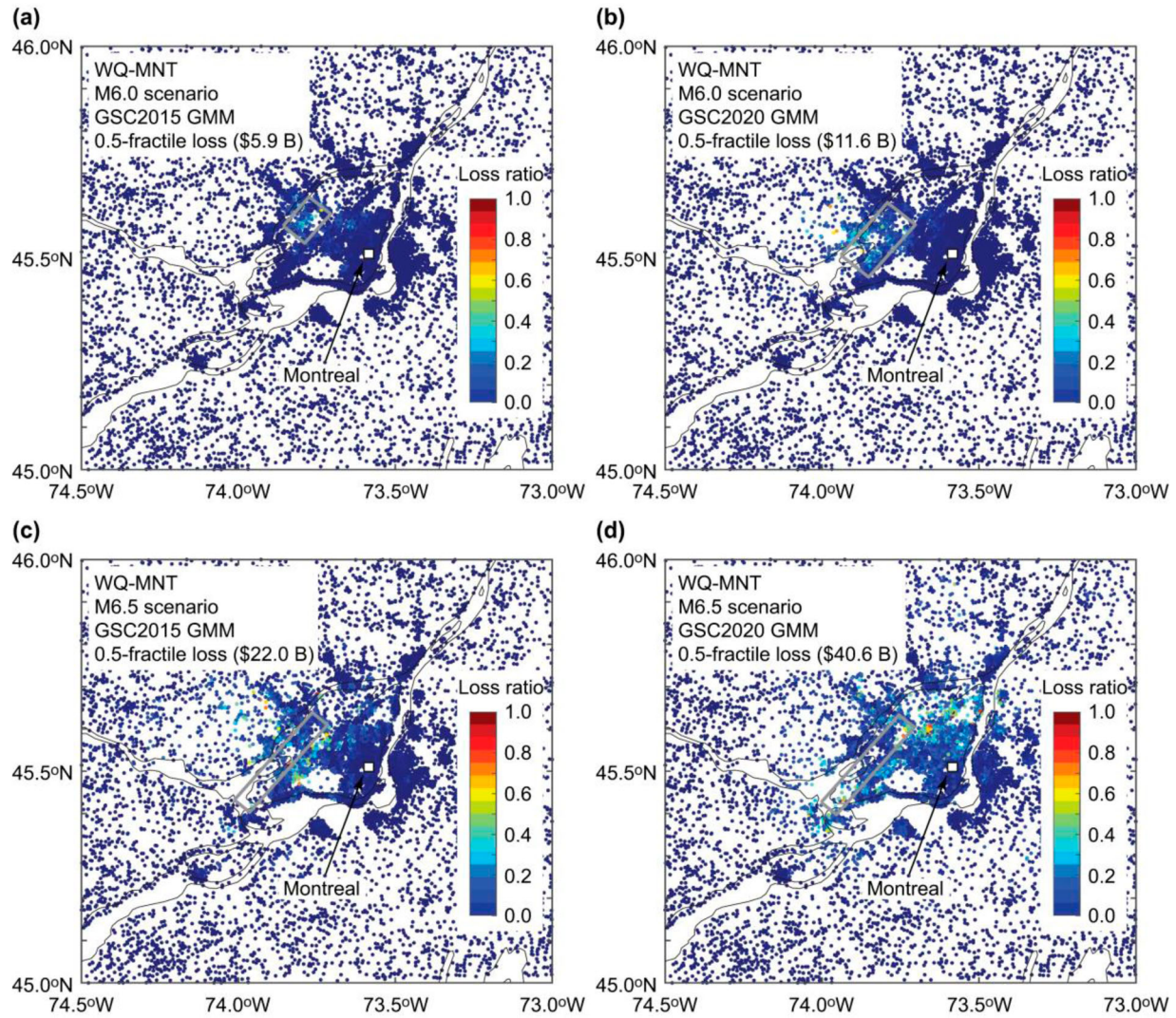
Figure 18. Seismic loss ratio maps for the 0.5-fractile (median) seismic loss scenarios for the WQ-MNT source by considering two scenario magnitudes (M6.0 [a,b] and M6.5 [c,d]) and two ground motion models (GSC2015 [a,c] and GSC2020 [b,d]). The grey rectangles are the fault plane boundaries of the stochastic source models.

the size of the fault rupture plane becomes larger according to the scaling relationships, and when the earthquake magnitude is smaller, the position of the fault rupture plane floats more freely within the overall fault plane boundary. In other words, when the earthquake magnitude is smaller, there is more uncertainty as to whether the event hits or misses urban areas. The effects of different ground motion models on the shake maps can be seen by comparing the left and right columns of Figure 13. Generally speaking, the GSC2020 model generates higher ground motions, especially distances up to 50 km from the fault rupture plane (Figure 6).

Figure 14 shows the corresponding seismic loss ratio maps for the WQ-PEM source by considering the three scenario magnitudes and two ground motion models. It is noted that the loss ratio at a given location is calculated as total seismic loss divided by total asset value.

As expected, the spatial patterns of the shake maps and loss ratio maps are similar. It is important to note that although the occurrence of major loss events reaching tens of billions of dollars is rare (below 10^{-3} probability level; Figure 9), when they occur, the economic consequences of the events can be devastating (e.g. a typical M6.5 event could cause C\$4 to C\$10 billion loss, while a typical M7.0 event could cause C\$16 to C\$32 billion loss; Figure 14).

3.2.2 Critical scenarios near Montreal

The similar seismic loss estimation is performed by considering the M6.0 and M6.5 scenarios from the WQ-MNT source (Figure 5(c)). Note that the M7.0 scenario is not considered for the WQ-MNT due to the shorter fault trace. The conditional probability distributions of SA at 0.3 s at a site in Montreal and portfolio seismic

loss are shown in Figure 15 and 16, respectively, whereas the shake maps and seismic loss ratio maps of the 0.5-fractile seismic loss scenarios are shown in Figures 17 and 18, respectively. The observations that are mentioned for the WQ-PEM source in Section 3.2.1 are generally applicable to the WQ-MNT source, and thus these are not repeated here.

A striking difference of the two scenario-based loss estimation is that for the same magnitude, the portfolio seismic loss for the WQ-MNT is significantly greater than that for the WQ-PEM. For instance, the median portfolio losses for the M6.5 WQ-MNT scenarios are C$22.0 and C$40.6 billion when the GSC2015 and GSC2020 ground motion models are adopted, respectively (Figure 18(c and d)). In contrast, these median values for the WQ-PEM scenarios are C$4.0 and C$9.5 billion (Figure 14(c and d)). The main cause of the differences is the spatial density of the buildings in the vicinity of the considered fault sources. The interaction between the earthquake sources and the building exposures needs to be carefully considered when regional seismic risk management is focused upon.

4. Conclusions

The quantification of regional earthquake risk is an essential first step for effective seismic risk management. Yet, such assessments have been lacking in eastern Canada. This study conducted two types of seismic loss estimation for residential wooden buildings in the WQSZ, where two important cities, Ottawa and Montreal, are located. The first regional seismic loss model used a stochastic event set generated from the GSC's seismic hazard model and facilitated the calculation of the EP curve. The second regional seismic loss model adopted a stochastic source modelling method to develop conditional probability distributions of scenario-based regional seismic loss as well as critical shake and seismic loss maps. An explicit consideration of finite-fault rupture scenarios was a major advancement of the regional seismic risk assessments in eastern Canada. It was important to use these two seismic loss models jointly for earthquake risk management.

The numerical results that were obtained for the WQSZ and for urban areas near Ottawa and Montreal indicated that the overall financial seismic risk for the region at practical probability levels, such as 0.002 annual probability of exceedance or 1-in-500 years return period, is in the range of C$10 billion or less. However, there is possibility that more devastating earthquake disasters, reaching tens of billions of dollars, could be triggered, when moderate-to-large earthquakes strike near Ottawa or Montreal. It is important to note that the low probability of the major seismic loss is due to the low probability of earthquake occurrence, but when such an earthquake occurs, the regional impact of the event can be significant due to high exposure and high vulnerability of the existing building stock in the region.

Lastly, it is important to point out the limitations of the current study. The finite-fault source modelling that was performed in this study is only the first step towards a more accurate fault rupture characterisation, and alternative values for the finite-fault sources should be considered in the future study. The adopted building and vulnerability databases, created by the GSC, are comprehensive but their accuracy may be low, when compared to locally compiled building exposure data, such as those used for the metropolitan region of Montreal (Rosset et al. 2019, 2022). When damage data become available from future earthquakes or high-quality experimental data are produced in structural laboratories, comparative studies are highly desirable to validate the GSC's vulnerability functions. Moreover, the local site parameters that are obtained from the global V_{S30} database are crude and lack local resolutions, compared to microzonation maps produced by Rosset, Bour-Belvaux, and Chouinard (2015) in the same region. A systematic comparison between the regional seismic loss estimation as conducted in this study and the more detailed seismic loss estimation would be a useful investigation to quantify the model uncertainty in the seismic loss estimation.

ORCID

Jeremy Rimando 🔵 http://orcid.org/0000-0003-2437-4579
Alexander L. Peace 🔵 http://orcid.org/0000-0001-7846-3898
Philippe Rosset 🔵 http://orcid.org/0000-0002-7596-9196

References

Adams, J., G. C. Rogers, S. Halchuk, D. McCormack, and J. Cassidy. 2002. "The Case of an Advanced National Earthquake Monitoring System for Canada's cities at risk." In: *Proceedings of the 7th U.S. National Conference on Earthquake Engineering*, Boston, United States, 10 p.

AIR Worldwide. 2013. *Study of Impact and the Insurance and Economic Cost of a Major Earthquake in British Columbia and Ontario/Québec*, 264 p.

Atkinson, G. M., and J. Adams. 2013. "Ground Motion Prediction Equations for Application to the 2015 Canadian National Seismic Hazard Maps." *Canadian Journal of Civil Engineering* 40: 988–998. doi:10.1139/cjce-2012-0544.

Baker, J. W., B. Bradley, and P. Stafford. 2021. *Seismic Hazard and Risk Analysis*. Cambridge, United Kingdom: Cambridge University Press.

Cassidy, J. F., G. C. Rogers, M. Lamontagne, S. Halchuk, and J. Adams. 2010. "Canada's Earthquakes: The Good, the Bad, and the Ugly." *Geoscience Canada* 37: 1–16. https://journals.lib.unb.ca/index.php/GC/article/view/15300

Foulser-Piggott, R., G. Bowman, and M. Hughes. 2020. "A Framework for Understanding Uncertainty in Seismic Risk Assessment." *Risk Analysis* 40: 169–182. doi:10.1111/risa.12919.

Ghofrani, H., G. M. Atkinson, L. Chouinard, P. Rosset, and K. F. Tiampo. 2015. "Scenario Shakemaps for Montreal." *Canadian Journal of Civil Engineering* 42: 463–476. doi:10.1139/cjce-2014-0496.

Goda, K. 2017. "Probabilistic Characterization of Seismic Ground Deformation due to Tectonic Fault Movements." *Soil Dynamics and Earthquake Engineering* 100: 316–329. doi:10.1016/j.soildyn.2017.05.039.

Goda, K. 2019. "Nationwide Earthquake Risk Model for Wood-Frame Houses in Canada." *Frontiers in Built Environment* 5: 128. doi:10.3389/fbuil.2019.00128.

Goda, K., and G. M. Atkinson. 2010. "Intraevent Spatial Correlation of Ground-Motion Parameters Using SK-net Data." *Bulletin of the Seismological Society of America* 100: 3055–3067. doi:10.1785/0120100031.

Goda, K., and H. P. Hong. 2009. "Deaggregation of Seismic Loss of Spatially Distributed Buildings." *Bulletin of Earthquake Engineering* 7: 255–272. doi:10.1007/s10518-008-9093-2.

Goulet, C. A., Y. Bozorgnia, N. Kuehn, L. Al Atik, R. R. Youngs, R. W. Graves, and G. M. Atkinson. 2017. "NGA-East Ground-Motion Models for the U.S. Geological Survey National Seismic Hazard Maps." PEER Report No. 2017/03, 180 p.

Halchuk, S. 2009. "Seismic Hazard Earthquake Epicentre File (SHEEF) Used in the 4th Generation Seismic Hazard Maps of Canada." *Geological Survey of Canada Open File* 6208: 16. doi:10.4095/261333.

Halchuk, S., T. I. Allen, J. Adams, and G. C. Rogers. 2014. "Fifth Generation Seismic Hazard Model Input Files as Proposed to Produce Values for the 2015 National Building Code of Canada." *Geological Survey of Canada Open File* 7576: 15. doi:10.4095/293907.

Heath, D. C., D. J. Wald, C. B. Worden, E. M. Thompson, and G. M. Smoczyk. 2020. "A Global Hybrid VS30 map with a Topographic Slope–Based Default and Regional map Insets." *Earthquake Spectra* 36: 1570–1584. doi:10.1177/8755293020911137.

Hobbs, T., J. M. Journeay, and P. LeSueur. 2021. "Developing a Retrofit Scheme for Canada's Seismic Risk Model." *Geological Survey of Canada Open File* 8822: 10. doi:10.4095/328860.

Hyndman, R. D., and G. C. Rogers. 2010. "Great Earthquakes on Canada's West Coast: A Review." *Canadian Journal of Earth Sciences* 47: 801–820. doi:10.1139/E10-0.

Kolaj, M., S. Halchuk, J. Adams, and T. I. Allen. 2020. "Sixth Generation Seismic Hazard Model of Canada: Input Files to Produce Values Proposed for the 2020 National Building Code of Canada; Geological Survey of Canada." *Open File* 8630. 15 p. doi:10.4095/327322.

Lamontagne, M., P. Brouillette, S. Grégoire, M. P. Bédard, and W. Bleeker. 2020. "Faults and Lineaments of the Western Quebec Seismic Zone, Quebec and Ontario. Geological Survey of Canada." *Open File* 8361. doi:10.4095/321900.

Mai, P. M., and G. C. Beroza. 2002. "A Spatial Random Field Model to Characterize Complexity in Earthquake Slip." *Journal of Geophysical Research: Solid Earth* 107: ESE 10. doi:10.1029/2001JB000588.

Mai, P. M., P. Spudich, and J. Boatwright. 2005. "Hypocenter Locations in Finite-Source Rupture Models." *Bulletin of the Seismological Society of America* 95: 965–980. doi:10.1785/0120040111.

Mazzotti, S., and J. Townend. 2010. "State of Stress in Central and Eastern North American Seismic Zones." *Lithosphere* 2: 76–83. doi:10.1130/L65.1.

Mitchell-Wallace, K., M. Jones, J. Hillier, and M. Foote. 2017. *Natural Catastrophe Risk Management and Modelling: A Practitioner's Guide*, 536 p. Chichester, UK: Wiley-Blackwell.

Morell, K. D., R. Styron, M. Stirling, J. Griffin, R. Archuleta, and T. Onur. 2020. "Seismic Hazard Analyses from Geologic and Geomorphic Data: Current and Future Challenges." *Tectonics* 39: 1–47. doi:10.1029/2018TC005365.

Morris, A., D. A. Ferrill, and D. B. Henderson. 1996. "Slip-tendency Analysis and Fault Reactivation." *Geology* 24: 275–278. doi:10.1130/0091-7613(1996)024<0275:STAAFR>2.3.CO;2.

Peace, A. L., K. J. W. McCaffrey, J. Imber, J. Hunen, R. van Hobbs, and R. Wilson. 2018. "The Role of pre-Existing Structures During Rifting, Continental Breakup and Transform System Development, Offshore West Greenland." *Basin Research* 30: 373–394. doi:10.1111/bre.12257.

Rimando, J., and A. Peace. 2021. "Reactivation Potential of Intraplate Faults in the Western Quebec Seismic Zone." *Eastern Canada. Earth and Space Science* 8: e2021EA001825. doi:10.1029/2021EA001825.

Rosset, P., M. Bour-Belvaux, and L. Chouinard. 2015. "Estimation and Comparison of Vs30 Microzonation Maps for Montreal Using Multiple Sources of Information." *Bulletin of Earthquake Engineering* 13 (8): 2225–2239. doi:10.1007/s10518-014-9716-8.

Rosset, P., and Chouinard, L.E. 2009. "Characterization of Site Effects in Montreal, Canada." *Natural Hazards* 48: 295–308. doi:10.1007/s11069-008-9263-1.

Rosset, P., L. Chouinard, and M. J. Nollet. 2022. "Consequences on Residential Buildings in Greater Montreal for a Repeat of the 1732 M5.8 Montreal Earthquake." In: *Proceedings of the Canadian Society of Civil Engineering Annual Conference 2021* (*CSCE 2021*), 667–679. doi: 10.1007/978-981-19-0507-0_58.

Rosset, P., M. Kert, S. Youance, M. J. Nollet, and L. Chouinard. 2019. "Could Montreal Residential Buildings

Suffer Important Losses in Case of Major Earthquakes?" In: *Proceedings of the 12th Canadian Conference on Earthquake Engineering*, Quebec City, 7 p.

Thingbaijam, K. K. S., P. M. Mai, and K. Goda. 2017. "New Empirical Earthquake Source-Scaling Laws." *Bulletin of the Seismological Society of America* 107: 2225–2246. doi:10.1785/0120170017.

Ulmi, M., C. L. Wagner, M. Wojtarowicz, J. L. Bancroft, N. L. Hastings, W. Chow, J. R. Rivard, et al. 2014. "Hazus-MH 2.1 Canada User and Technical Manual: Earthquake Module. Geological Survey of Canada." *Open File* 7474: 245. doi:10.4095/293800.

Wald, D. J., and T. I. Allen. 2007. "Topographic Slope as a Proxy for Seismic Site Conditions and Amplification." *Bulletin of the Seismological Society of America* 97: 1379–1395. doi:10.1785/0120060267.

Wesson, R. L., D. M. Perkins, E. V. Leyendecker, R. J. Jr. Roth, and M. D. Petersen. 2004. "Losses to Single-Family Housing from Ground Motions in the 1994 Northridge, California, Earthquake." *Earthquake Spectra* 20: 1021–1045. doi:10.1193/1.1775238.

Yu, K., P. Rosset, and L. E. Chouinard. 2016. "Seismic Vulnerability Assessment for Montreal." *Georisk* 10 (2): 164–178. doi:10.1080/17499518.2015.1106562.